Corrections

NEUROSCIENCE

Correction for "Anterograde or retrograde transsynaptic labeling of CNS neurons with vesicular stomatitis virus vectors," by Kevin T. Beier, Arpiar Saunders, Ian A. Oldenburg, Kazunari Miyamichi, Nazia Akhtar, Liqun Luo, Sean P. J. Whelan, Bernardo Sabatini, and Constance L. Cepko, which appeared in issue 37, September 13, 2011, of *Proc Natl Acad Sci USA* (108:15414–15419; first published August 8, 2011; 10.1073/pnas.1110854108).

The authors note the following: "Shortly after publication of the above manuscript, the replication-competent virus stock, vesicular stomatitis virus (VSV) (LCMV-G), used for the experiments in the paper, was found to be contaminated with wild type VSV [referred to as VSV (VSV-G)]. In addition, the replication-incompetent stock, VSV ΔG (LCMV-G) stock, only used for the data in Fig. 3*B*, was also contaminated by the same wild type VSV. When a pure stock of VSV (LCMV-G) was made, it was found to give inefficient anterograde transmission, in contrast to the efficient anterograde transmission seen with the mixed stock. Most cells infected with the pure VSV (LCMV-G) stock at an initial inoculation site were glia, although the virus did transmit anterogradely to a small number of neurons. The original VSV (VSV-G) stock used for the experiments published in the paper, which contaminated the VSV (LCMV-G) stock, was found to give efficient and specific anterograde transmission. The anterograde transmission was for all injections made directly into the brain, including from the caudate putamen to all of the anterograde target locations published in our paper. Moreover, it did not give retrograde labeling (e.g., see Fig. 2*A*). However, neither the original VSV (VSV-G) stock, nor an independent VSV (VSV-G) stock obtained from another lab, were found to give anterograde tracing from the eye, or from the nose, to the brain, when inoculated into either of these peripheral locations. The anterograde tracing from the eye or nose to the brain was only seen in our initial studies using the mixed stock, and in our repeated set of experiments with this same mixed stock. We have since plaque purified viruses from this mixed stock. We tested 21 plaque purified viruses for their ability to give anterograde tracing from a peripheral injection site by injecting into the eye and examining the brains. Several stocks from plaque-purified viruses gave such anterograde transmission, and all of these viruses encoded VSV-G only (i.e., not LCMV-G) (for an example, see Fig. A). These same stocks also give the anterograde tracing patterns seen from inoculations of the caudate-putamen (similar to patterns shown in Fig. 3). We are now studying these VSV-G viruses to determine why they are such effective anterograde tracers, and why individual stocks differ when injected into peripheral sites. The differences may be due to the fact that injecting a peripheral site demands long distance travel from the initially infected cells to the brain, or it may have more to do with some other aspect of the sites being peripheral to the brain.

"For those neuroscientists wishing to perform anterograde, polysynaptic tracing, we recommend using the VSV (VSV-G) stock that we have plaque purified. For monosynaptic tracing, the ΔG VSV genome can be used with any of the viral G proteins published in PNAS: VSV-G (for anterograde), LCMV-G (for anterograde), or RABV-G (for retrograde). It may be the case that VSV-G is more efficient for anterograde monosynaptic tracing than LCMV-G. More testing needs to be done, particularly in vivo, to determine the relative efficiencies of these G proteins for monosynaptic tracing.

"We stand by the conclusions of the paper that VSV is an effective transsynaptic tracer, and that the G protein determines the direction of transmission. The RABV-G gives retrograde transmission, while the VSV-G and the LCMV-G direct anterograde transmission, with the VSV-G giving more efficient transmission than LCMV-G as a replication-competent virus."

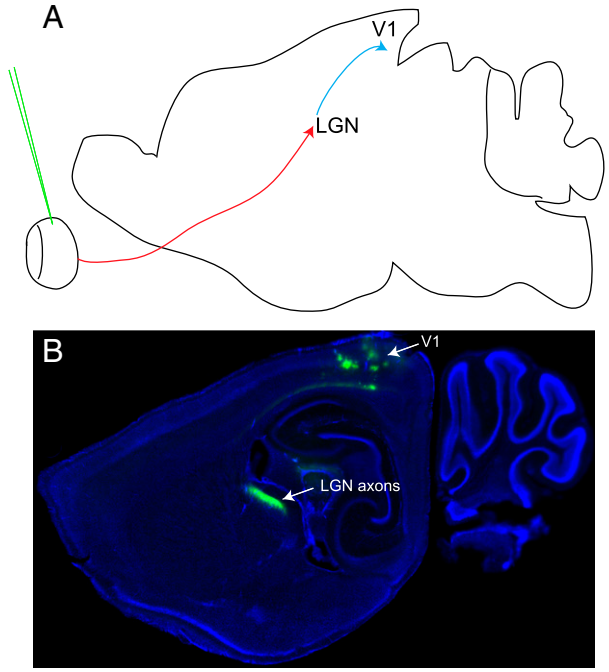

Fig. A. Anterograde pattern of spread of VSV (VSV-G) from a virus stock derived from a purified plaque. Anterograde transmission was tested by injection into the vitreous body of the eye. (*A*) A diagram of a parasaggital section of the brain illustrates the expected pattern of transmission for an anterograde transsynaptic virus injected into the eye. It would be expected to label several brain centers involved in visual processing, including the lateral geniculate nucleus (LGN) and visual cortex area 1 (V1). The red arrow indicates the path of the retinal ganglion cell axons to their direct targets, the cells of the LGN. The blue arrow indicates the path of the LGN axons to their V1 targets. The green needle indicates the injection site. (*B*) A parasaggital section from an injected brain at 7 d post infection, showing labeling of the LGN and V1. All injections that gave brain labeling using this virus stock showed a similar pattern (5/10 animals injected).

www.pnas.org/cgi/doi/10.1073/pnas.1207087109

CELL BIOLOGY

Correction for "Wnt signaling and a Smad pathway blockade direct the differentiation of human pluripotent stem cells to multipotent neural crest cells," by Laura Menendez, Tatiana A. Yatskievych, Parker B. Antin, and Stephen Dalton, which appeared in issue 48, November 29, 2011, of *Proc Natl Acad Sci USA* (108:19240–19245; first published November 14, 2011; 10.1073/pnas.1113746108).

The authors note that they omitted a reference to an article by Wang et al. The complete reference appears below.

Additionally, the authors note that on page 19245, left column, third full paragraph, lines 1–6, "WA09 (WiCell), RUES1, RUES2 (A. Brivanlou, The Rockefeller University, New York) hESCs, and the hiPSC lines Fib2-iPS4 and Fib2-iPS5 (George Daley, Children's Hospital, Boston) were cultured on Geltrex-coated plates (Invitrogen) in chemically defined media containing Heregulin β (10 ng/mL), Activin A (10 ng/mL), LR-Igf (200 ng/mL), and Fgf2 (8 ng/mL) as described previously (24)" should instead appear as "WA09 (WiCell), RUES1, RUES2 (A. Brivanlou, The Rockefeller University, New York) hESCs, and the hiPSC lines Fib2-iPS4 and Fib2-iPS5 (George Daley, Children's Hospital, Boston) were cultured on Geltrex-coated plates (Invitrogen) in chemically defined media containing Heregulin β (10 ng/mL), Activin A (10 ng/mL), LR-Igf (200 ng/mL), and Fgf2 (8 ng/mL) as described previously (25)."

25. Wang L, et al. (2007) Self-renewal of human embryonic stem cells requires insulin-like growth factor-1 receptor and ERBB2 receptor signaling. *Blood* 110:4111–4119.

www.pnas.org/cgi/doi/10.1073/pnas.1207810109

APPLIED BIOLOGICAL SCIENCES, ENGINEERING

Correction for "Supramolecular nanostructures that mimic VEGF as a strategy for ischemic tissue repair," by Matthew J. Webber, Jörn Tongers, Christina J. Newcomb, Katja-Theres Marquardt, Johann Bauersachs, Douglas W. Losordo, and Samuel I. Stupp, which appeared in issue 33, August 16, 2011, of *Proc Natl Acad Sci USA* (108:13438–13443; first published August 1, 2011; 10.1073/pnas.1016546108).

The authors note that the following statement should be added to the Acknowledgments: "Funding was also provided by NIH Grants HL-095874 and P01HL-108795."

www.pnas.org/cgi/doi/10.1073/pnas.1207994109

MEDICAL SCIENCES

Correction for "Glucocerebrosidase gene-deficient mouse recapitulates Gaucher disease displaying cellular and molecular dysregulation beyond the macrophage," by Pramod K. Mistry, Jun Liu, Mei Yang, Timothy Nottoli, James McGrath, Dhanpat Jain, Kate Zhang, Joan Keutzer, Wei-Lein Chuang, Wajahat Z. Mehal, Hongyu Zhao, Aiping Lin, Shrikant Mane, Xuan Liu, Yuan Z. Peng, Jian H. Li, Manasi Agrawal, Ling-Ling Zhu, Harry C. Blair, Lisa J. Robinson, Jameel Iqbal, Li Sun, and Mone Zaidi, which appeared in issue 45, November 9, 2010, of *Proc Natl Acad Sci USA* (107:19473–19478; first published October 20, 2010; 10.1073/pnas.1003308107).

The authors note that the author name Wei-Lein Chuang should instead appear as Wei-Lien Chuang. The corrected author line appears below. The online version has been corrected.

Pramod K. Mistry, Jun Liu, Mei Yang, Timothy Nottoli, James McGrath, Dhanpat Jain, Kate Zhang, Joan Keutzer, Wei-Lien Chuang, Wajahat Z. Mehal, Hongyu Zhao, Aiping Lin, Shrikant Mane, Xuan Liu, Yuan Z. Peng, Jian H. Li, Manasi Agrawal, Ling-Ling Zhu, Harry C. Blair, Lisa J. Robinson, Jameel Iqbal, Li Sun, and Mone Zaidi

www.pnas.org/cgi/doi/10.1073/pnas.1207533109

BIOPHYSICS AND COMPUTATIONAL BIOLOGY, CHEMISTRY

Correction for "Ligand binding to protein-binding pockets with wet and dry regions," by Lingle Wang, B. J. Berne, and R. A. Friesner, which appeared in issue 4, January 25, 2011, of *Proc Natl Acad Sci USA* (108:1326–1330; first published January 4, 2011; 10.1073/pnas.1016793108).

The authors note that their conflict of interest statement was omitted during publication. The authors declare that R.A.F. is a founder of Schrodinger, Inc.

www.pnas.org/cgi/doi/10.1073/pnas.1207504109

Anterograde or retrograde transsynaptic labeling of CNS neurons with vesicular stomatitis virus vectors

Kevin T. Beier[a,b,c], Arpiar Saunders[c,d], Ian A. Oldenburg[c,d], Kazunari Miyamichi[e,f], Nazia Akhtar[c,d], Liqun Luo[e,f], Sean P. J. Whelan[g], Bernardo Sabatini[c,d], and Constance L. Cepko[a,b,c,1]

Departments of [a]Genetics, [b]Ophthalmology, [d]Neurobiology, and [g]Microbiology and Molecular Genetics and [c]Howard Hughes Medical Institute, Harvard Medical School, Boston, MA 02115; and [e]Department of Biology and [f]Howard Hughes Medical Institute, Stanford University, Stanford, CA 94305

Contributed by Constance L. Cepko, July 7, 2011 (sent for review June 10, 2011)

To understand how the nervous system processes information, a map of the connections among neurons would be of great benefit. Here we describe the use of vesicular stomatitis virus (VSV) for tracing neuronal connections in vivo. We made VSV vectors that used glycoprotein (G) genes from several other viruses. The G protein from lymphocytic choriomeningitis virus endowed VSV with the ability to spread transsynaptically, specifically in an anterograde direction, whereas the rabies virus glycoprotein gave a specifically retrograde transsynaptic pattern. The use of an avian G protein fusion allowed specific targeting of cells expressing an avian receptor, which allowed a demonstration of monosynaptic anterograde tracing from defined cells. Synaptic connectivity of pairs of virally labeled cells was demonstrated by using slice cultures and electrophysiology. In vivo infections of several areas in the mouse brain led to the predicted patterns of spread for anterograde or retrograde tracers.

Defining the connections among neurons will be necessary in order to fully understand the information transformations carried out by the nervous system. Ideally, a method for this task would be rapid and straightforward in its application, could be delivered in vivo to most or all locations, and could be used ex vivo in slice or explant cultures. It would also show synaptic specificity but not be diluted as it moved across synapses. Finally, it would be most useful if it not only enabled the mapping of connections, but also provided a way to study the function of connected neurons.

Viruses not only have features that allow for the tracing of neuronal connections, but they provide a platform for functional studies by virtue of their ability to transduce genes. Two neurotropic viruses, the pseudorabies virus (PRV) (1) and the rabies virus (RABV) (2), have been the most extensively used to map neural connections. The Bartha strain of PRV, a type of herpes virus, moves in the retrograde direction (3), whereas the H129 strain of the herpes simplex virus (HSV) moves only anterogradely (4). HSVs are large and complex viruses, making them difficult to engineer, and the commonly used strains have a limited tropism. RABV exhibits exclusively retrograde transsynaptic spread and has recently been modified to be safer for laboratory applications by deletion of the rabies RABV-G gene (5). This glycoprotein (G)-deleted form of RABV allows targeting of RABV to specific cells through the use of the extracellular domain of a different G protein, the avian sarcoma and leukosis virus A protein [ASLV (A)], which targets infection to cells expressing its receptor, tumor virus A (TVA), normally found only in avian species (6).

As an alternative viral vector for neural tracing, we wished to use a virus that is straightforward to engineer, relatively safe for laboratory personnel, and very flexible regarding its acceptance of G proteins from other viruses. This latter goal was in the hope of being able to rationally design viruses that would transmit transsynaptically in defined directions. We turned to vesicular stomatitis virus (VSV), a negative strand RNA virus that is a member of the *Rhabdoviridae* family (7). Its use as a gene transfer agent in the CNS had already been established (8), although its native G protein, VSV-G, did not promote specific transsynaptic spread. VSV is lethal to individual cells, and to an animal when injected into the brain, but it is significantly less toxic after natural infections in humans and is being developed as a vaccine vector for humans (9). In addition, VSV has demonstrated great versatility in its ability to be pseudotyped with other virus' glycoproteins (10–13), and its genome has been successfully engineered by using straightforward manipulations (14).

We successfully created VSV vectors encoding one of several glycoproteins. These include the RABV-G and the G from an arenavirus, lymphocytic choriomeningitis virus (LCMV). Injecting these viruses into the murine CNS led to directionally selective, transsynaptic spread along anatomically defined pathways, across several synapses. We also show that these VSV vectors can be used for monosynaptic tracing, in the same way as the monosynaptic tracing version of RABV. However, through the use of LCMV-G, these VSV vectors have the additional ability to monosynaptically, or polysynaptically, trace circuits in an exclusively anterograde direction. Additionally, these vectors can use the ASLV-A/RABV-G fusion protein (15) to specifically target TVA-expressing cells. These efforts will be augmented by the use of a newly created conditional TVA line of mice (16), wherein specific Cre drivers can be used to direct targeting of specific populations of cells in vivo.

Results

VSV with LCMV-G Is a Transsynaptic Anterograde Tracer. To determine whether VSV could be engineered to travel transsynaptically in an anterograde direction, we created a VSV with the LCMV-G gene positioned within the viral genome in place of the VSV-G gene and with YFP inserted into the first position [VSV (LCMV-G)] (Fig. 1). To test for retrograde spread, it was injected into the lateral geniculate nucleus (LGN), and the number of labeled retinal ganglion cells (RGCs) was quantified and compared with the number labeled after LGN injection of VSV encoding RABV-G [VSV(RABV-G)] or VSV-G(VSV) (Fig. 2*A*). Although many cells were labeled by VSV(RABV-G), as might be predicted for a virus with RABV-G, no RGCs were labeled by VSV using its own G protein. Few RGCs were labeled with VSV(LCMV-G). These might indicate a severely reduced retrograde transmission property of the virus. Alternatively, they might reflect circuits involving a small region of the LGN, the intergeniculate leaflet (IGL), that project to the retina via autonomic circuits (17), or retinopetal projections from histaminergic neurons of the hypothalamus (18) that might get input, directly or indirectly, from the LGN.

To compare anterograde spread of VSV with the three glycoproteins, mice were injected in the vitreous humor of the eye, where the virus could infect RGCs (Fig. 2*B*). YFP labeling was observed in the brains of 16/16 VSV(LCMV-G) infected mice,

Author contributions: K.T.B., A.S., B.S., and C.L.C. designed research; K.T.B., A.S., I.A.O., and N.A. performed research; K.T.B., A.S., N.A., and S.P.J.W. contributed new reagents/analytic tools; K.T.B., A.S., I.A.O., K.M., L.L., S.P.J.W., B.S., and C.L.C. analyzed data; and K.T.B. and C.L.C. wrote the paper.

The authors declare no conflict of interest.

Freely available online through the PNAS open access option.

Data deposition: The plasmids and their respective maps reported in this paper have been deposited in the Addgene Repository, http://www.addgene.org/pgvec1 (accession nos. 31832, 31833, 31834, 31842).

[1]To whom correspondence should be addressed. E-mail: cepko@genetics.med.harvard.edu.

This article contains supporting information online at www.pnas.org/lookup/suppl/doi:10.1073/pnas.1110854108/-/DCSupplemental.

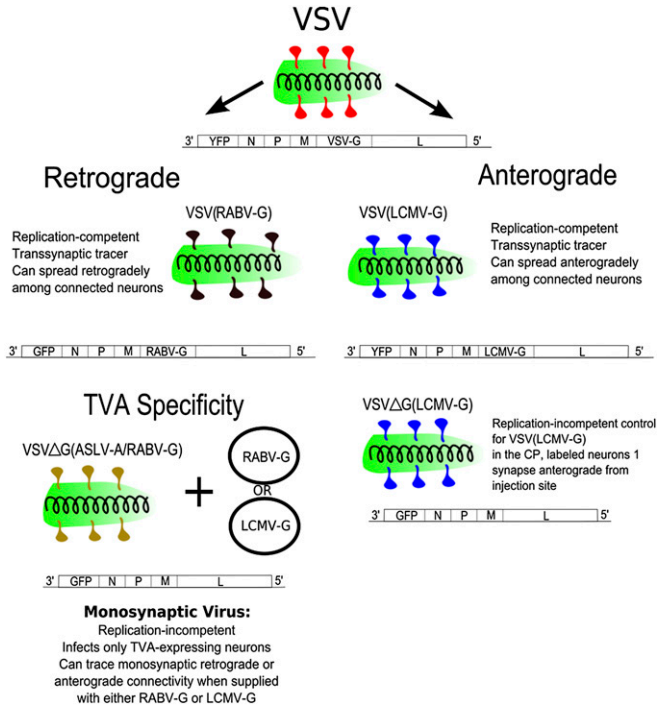

Fig. 1. The viruses used in this study. The glycoproteins used are diagrammed as follows: red, VSV-G; black, RABV-G; blue, LCMV-G; yellow, ASLV-A/RABV-G. The status of the G gene in the viral genome was as follows: ΔG, G gene is deleted; RABV-G and LCMV-G, G gene encoded in the viral genome (for the replication-competent viruses). The circles adjacent to VSVΔG(ASLV-A/RABV-G) indicate plasmid delivery of either RABV-G or LCMV-G for pseudotyping of the VSVΔG virus after infection of TVA-expressing cells by VSVΔG (ASLV-A/RABV-G).

but no fluorescent labeling was observed in mice injected with VSV (0/4). A very small number of cells in the IGL of the LGN and the suprachiasmatic nucleus (SCN) was seen in the case of VSV(RABV-G) (3/4), consistent with the observations after infections of the retrograde tracer, PRV-Bartha, into the eye (17).

YFP labeling was observed in both primary as well as secondary visual centers in mice infected subretinally in the eye with VSV(LCMV-G). These areas included the primary visual centers, LGN, superior colliculus (SC), and SCN in 16/16 animals; in 9/16 mice, labeling was also seen in visual cortex areas V1 and V2 (Fig. 2 *D–J* and Fig. S1) (19). Animals injected subretinally with a replication-incompetent (G deleted) VSV pseudotyped with LCMV-G [VSVΔG(LCMV-G)] did not show brain transmission ($n = 3$). The amount of YFP signal and cell health progressively decreased in the same order as the expected pattern of spread. Cell toxicity was seen a few days postinjection (dpi), consistent with previous reports (20). The number of cells labeled in the SCN, SC, and LGN was quantified 3–8 dpi (Table S1). At 3 dpi, the highest numbers were in the SCN. The number in the SCN began to decline by 6 dpi, likely due to viral toxicity. At 6 dpi, the number of labeled LGN and SC neurons increased. The longer lag to labeling of the LGN and SC may reflect the increased distance from the retina to these areas, relative to the SCN, as well as perhaps more extensive connectivity within these regions. A similar pattern of cortical labeling was observed from an LGN injection with VSV(LCMV-G) (Fig. S1 *C–E*).

Because the distance between the LGN and retina is relatively large, injections of VSV(LCMV-G) were made into the caudate putamen (CP) to probe whether shorter-distance retrograde transport could occur. The CP of adult mice was injected, and brains were harvested between 1 and 5 dpi, three mice per time point. Infection of the CP with VSV(LCMV-G) (Fig. 3 and Fig. S2) gave a very different labeling pattern from that observed after infection with VSV(RABV-G) (Fig. 3*H*). Extensive labeling with VSV(LCMV-G) was seen within the area of the inoculation and other areas, including areas to which the CP is known to project, such as the globus pallidus (GP) and subthalamic nucleus (STn). VSV(LCMV-G) appeared to travel transsynaptically at the rate of one synapse per day as evidenced by labeling in anterograde transsynaptic targets, such as the GP and STn, at 2 dpi, and SNr, at 3 dpi. Most importantly, the only labeling observed in the cortex was along the needle path (e.g., Fig. 3*F*). Even when 10 times the amount of VSV(LCMV-G) that resulted in the labeling shown in Fig. 3 was injected into the CP, resulting in the labeling of nearly the entire CP, no cortical cells were labeled outside of the needle track. In contrast, CP injection of VSV(RABV-G) led to more extensive labeling in the cortex (Fig. 3*H*), even with 100-fold less virus than that used for the inoculations shown in Fig. 3 *B–G*. With VSV(RABV-G), retrogradely connected regions, including the CP, nucleus basalis, cortex, and GP, were labeled (Fig. 3*H*).

Of additional interest was the labeling pattern of replication-incompetent, G-deleted VSV pseudotyped with LCMV-G [VSVΔG(LCMV-G)]. Unexpectedly, cells in areas that received anterograde projections from the injection site were labeled. Labeling in these cells would indicate which cells are able to take up the virus without the virus' ability to amplify its glycoprotein levels. The labeling patterns for the replication-incompetent VSV with LCMV-G vs. RABV-G were very distinct. Replication-incompetent VSV with LCMV-G infected cells anterograde from the site of injection, including cells in the GP and STn. The STn did not get labeled by VSVΔG(RABV-G), whereas areas that project to the CP, such as the cortex, did get labeled with VSVΔG (RABV-G) (data not shown).

To examine the ability of VSV(LCMV-G) to trace another circuit anterogradely, we injected the olfactory epithelium, where infection could initiate in peripheral olfactory receptor neurons (ORNs). A time course of infection was carried out over 1–6 dpi. Sparse labeling of axons from ORNs was observed in the nerve layer of the olfactory bulb (OB) at 1 dpi. No labeled cells were detected in other parts of the brain. Periglomerular (PG) cells of the OB started to be labeled at 2 dpi, which was followed by the labeling of mitral cells (MCs) in the OB at 3 dpi (Fig. 4*B*). The viral spread from the axonal termini of ORNs to PG cells, MCs, and granule cells (GCs) (Fig. 4*B*) is consistent with anterograde connections among these neurons (21) (Fig. 4*A*). The labeled PG cells and GCs often formed clusters, consistent with the columnar synaptic organization of the local connections in the OB (22). Some of the labeled GC clusters reached to the rostral end of rostral migratory stream (RMS; Fig. 4*B*). In the cortex, sparse populations of layer I neurons (mostly composed of GABAergic local interneurons) were first labeled in the anterior olfactory nucleus and anterior piriform cortex at 3 dpi. The cortical labeling was greatly expanded at 4–5 dpi, when clustered layer II/III pyramidal cells were intensively labeled (Fig. 4*D*). Such clusters were sporadically distributed in the anterior piriform cortex, often, although not always, associated with labeled layer I neurons. This finding suggests that viral spread in this area could happen from layer I local inhibitory neurons to layer II/III pyramidal cells through the feedforward inhibitory circuit (23) (Fig. 4*C*). Labeling was not intensive in the posterior part of the cortex, including posterior piriform cortex and cortical amygdala. By 5–6 dpi, the virus spread was apparent in deeper brain areas, including septal and preoptic nuclei, periventricular and paraventricular nuclei, the arcuate hypothalamic nucleus, the habenular nucleus, and hippocampus (data not shown). These observations demonstrate that VSV(LCMV-G) can travel several synaptic steps from peripheral ORNs to the higher olfactory centers in an anterograde direction, as judged by known circuitry, and contrasts with studies using retrograde viruses (22, 24).

VSVΔG(LCMV-G) as a Monosynaptic Transsynaptic Anterograde Tracer. Wickersham et al. (15) created a powerful method for differentiating direct and indirect inputs by devising a method for labeling only direct connections using G-deleted RABV. To test whether VSV could be used in a similar manner, rat hippocampal slice cultures were transfected by using a gene gun with plasmids encoding the TVA receptor, RABV-G, and CFP (as a transfection

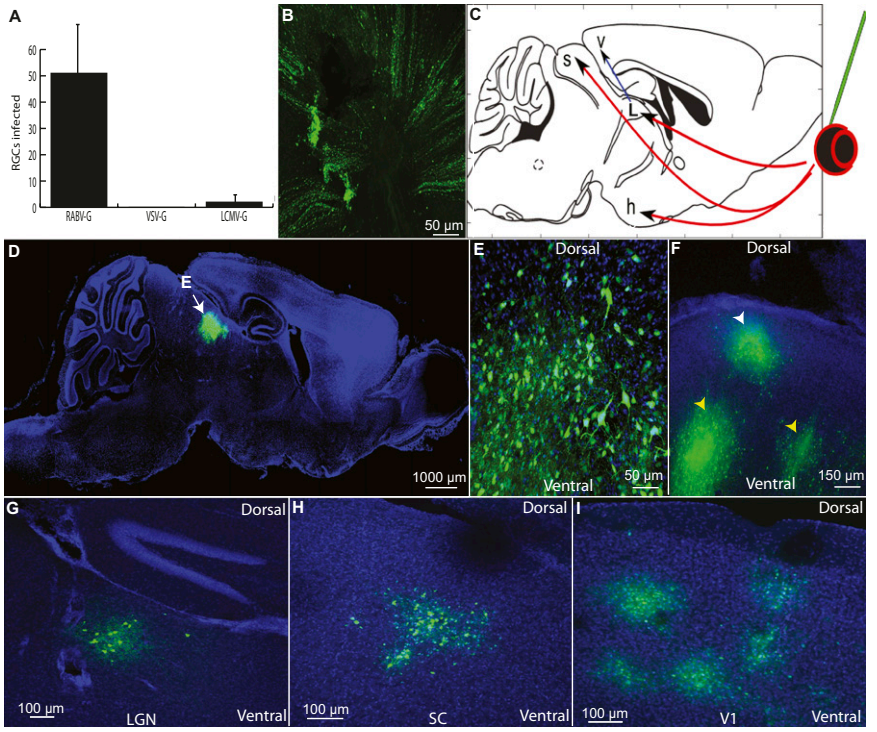

Fig. 2. Patterns of spread of VSV vectors injected into the eye and brain. (*A*) Retrograde transport of VSV was tested for VSV(RABV-G), WT VSV (which uses VSV-G), and VSV(LCMV-G) after injection into the LGN. The number of fluorescently labeled RGCs per retina at 4 dpi was counted (n = 4 animals for each virus). (Error bars: 1 SD.) (*B*) Anterograde transmission was tested by injection into the vitreous body of the eye. To determine whether RGCs were infected, RGC axons were examined and found to be fluorescently labeled after viral injection, as shown by an image taken at the optic nerve head of a VSV(LCMV-G)-infected retina 4 dpi. (*C*) An anterograde transsynaptic virus injected into the retina would be expected to label several brain centers involved in visual processing by anterograde spread, including the hypothalamus (h), LGN (L), SC (s), and V1 (v). Red arrows show direct targets of RGCs; blue indicates an indirect target; green indicates the injection site. (*D–F*) Parasaggital sections from brains after VSV(LCMV-G) injection into the eye. (*D* and *E*) In all mice injected in the eye subretinally, labeling in the brain was restricted to the visual system. At 7 dpi, strong labeling was observed in the deep layers of the SC (white arrow in *D*; high magnification shown in *E*). (*F*) A parasaggital section of the SC showing labeling in the more superficial layers (white arrowhead) and in the deeper layers (yellow arrowheads) at 6 dpi. Labeling was seen initially in the more superficial layers at 3 dpi and then in deeper layers at later times. (*G–I*) Primary retinorecipient areas (LGN, SC, SCN) and secondary (V1) visual centers were labeled after infection of the eye by VSV(LCMV-G), but not by the other viruses. Labeled nuclei 4 dpi included the LGN (*G*), SC (*H*), and V1 (*I*). (Images are from the same brain.) *C* is adapted from Franklin & Paxinos (56).

marker). One day after transfection, cultures were infected with a replication-incompetent VSV pseudotyped with the ASLV-A/RABV-G fusion protein, which directs infection specifically to TVA-expressing cells. Using a G-deleted mCherry-expressing VSV (VSVΔG), we observed infection of TVA-expressing neurons 18 h postinjection (hpi), identifiable as $mCherry^+/CFP^+$ (Fig. 5*A*), as well as upstream neurons (Fig. 5*B*). In control cultures that were not transfected, occasional cells were infected if 100 times more virus was used, but there was no spread from these cells, because they remained as single, isolated, labeled cells (data not shown).

A similar experiment was conducted by using LCMV-G in place of RABV-G. Rat hippocampal cultures were transfected with plasmids encoding the TVA receptor, LCMV-G, and ChR2-mCherry. One day after transfection, cultures were infected with a GFP-encoding VSVΔG pseudotyped with the ASLV-A/RABV-G protein. We observed infection specifically of TVA-expressing neurons ($GFP^+/mCherry^+$), and there was spread to nontransfected downstream neurons ($GFP^+/mCherry^-$) observable at 18 hpi (Fig. 5 *C–F*). The labeling patterns were consistent with synaptically restricted viral spread, as evidenced by juxtaposition in all cases of neuronal processes of transfected, infected cells with those that were infected, but not transfected (Fig. 5 *E* and *F*). The pattern of spread was different for viruses with the RABV-G vs. the LCMV-G protein. In pyramidal neurons with LCMV-G, transmission was not seen along the length of an axon, but rather only near the end of an axon, and there were few infected cells adjacent to the cell body or dendrites of a transfected cell. In contrast, there were many cells clustered near the cell bodies and dendrites of cells transmitting using the RABV-G (compare pattern of infected, but not transfected, cells in Fig. 5*B* and Fig. 5 *C* and *D*).

To determine whether pairs of cells labeled through viral transmission in the culture were synaptically connected, electrophysiological recordings were carried out (Fig. 5 *G–K*). A VSV with a point mutation in the M gene (M51R) (25, 26) was used for these experiments because this variant had been shown to prolong neuronal survival in hippocampal cultures (25). The cultures that were transfected with LCMV-G and ChR2 were used for this experiment, to allow light to be used to stimulate the transfected/infected neuron because of the presence of ChR2 (Fig. 5*H*). Infected, but not transfected, neurons that appeared near the axonal endings of the light-stimulated neuron were then examined for synaptic responses. As a control, other neurons that were uninfected, and that were in the vicinity of the infected but not transfected neuron, also were examined. Time-locked synaptic currents were recorded from 5/8 putative downstream infected neurons, whereas no currents were observed in noninfected cells from the same areas (0/10) (Fig. 5 *I–K*). These data indicate that the virus indeed spreads via synaptic connections.

Discussion

The goal of this work was to create a tracer that could move across multiple synapses specifically in an anterograde or retrograde direction, as well as to create a unique monosynaptic anterograde tracer. However, this work also revealed a fundamental aspect of viral transmission. The anterograde vs. retrograde properties of the VSV viruses with LCMV vs. RABV glycoproteins provide definitive evidence that directionality is a property of the G protein. This finding may be due to the sorting of the various glycoproteins into different vesicles in the Golgi, perhaps due to different sequences in the cytoplasmic tails of the glycoproteins (27). These viruses showed a broad host range in terms of cell types. The morphology of fluorescently-labeled cells suggested that GABAergic (e.g., GCs in the OB, medium spiny neurons), glutamatergic neurons (e.g., pyramidal cells in neocortex and piriform cortex, RGCs), and cholinergic cells (e.g., nucleus basalis neurons) (28) could be infected. Additionally, conventional axon–dendrite synapses, as well as dendrodendritic synapses (MC–GC interactions in the OB), were permissive for spread of VSV. Based on these labeling patterns, it appears that VSV may preferentially spread to GABAergic neurons, using either RABV-G or LCMV-G. Infection of local GABAergic neurons from cortical pyramidal neurons and the spread pattern from olfactory system injections suggest preferential labeling of GABAergic neurons.

The behavior of wild-type (WT) VSV in the CNS has been investigated. From intraocular injections of VSV, retinorecipient nuclei were labeled (29), implying anterograde transneuronal spread. However, retrograde viral spread also was likely, due to viral spread within the retina and infection of the contralateral

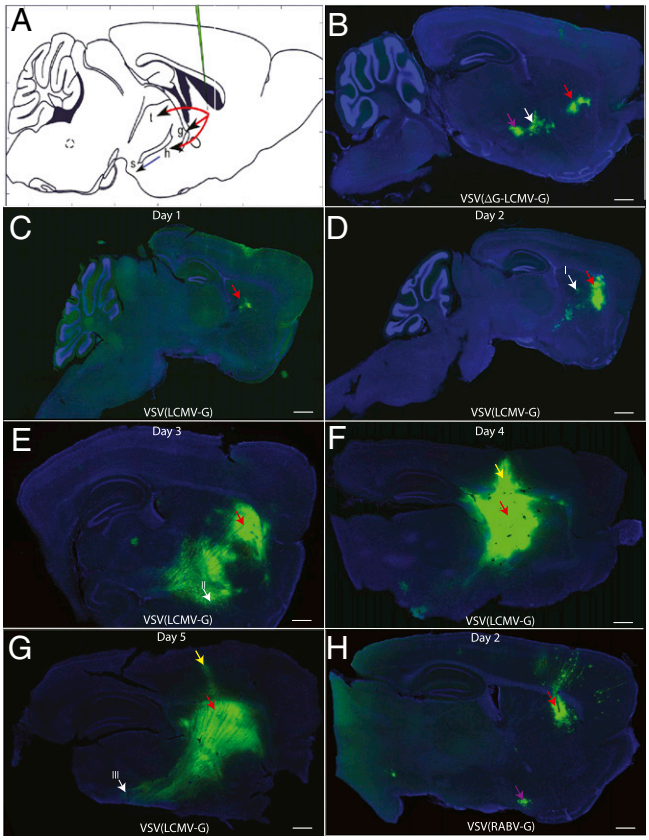

Fig. 3. Pattern of spread of VSV using LCMV-G and RABV-G after injection into the CP. (*A*) Expected targets for anterograde spread include the thalamus (t), GP (g), STn (h), and SNr (s) (red arrows, primary anterograde transsynaptic spread; blue, secondary anterograde spread; green, injection site). (*B*) Some of the direct anterograde targets were labeled with the replication-incompetent form, VSVΔG(LCMV-G), 4 dpi, including the GP (white arrow) and STn (purple arrow). (*C*–*G*) Replication-competent VSV (LCMV-G) was injected into the CP, and the time course of labeling was monitored for 5 d (*C*, 1 dpi; *D*, 2 dpi; *E*, 3 dpi; *F*, 4 dpi; *G*, 5 dpi). (*H*) The pattern of anterograde viral spread was distinct from that of retrograde spread, which was demonstrated by injection of VSV(RABV-G) into the CP, with the results shown at 2 dpi. The cortex exhibited many fluorescently labeled neurons, as did the nucleus basalis (purple arrow), which projects to the cortex, but not the CP. White arrows in *D*, *E*, and *G*, areas of high-magnification images (Fig. S2); red arrows, injection site; yellow arrows, leakage of virus along the needle path in *F* and *G*. (Scale bars: 1 mm.) *A* is adapted from Franklin & Paxinos (56).

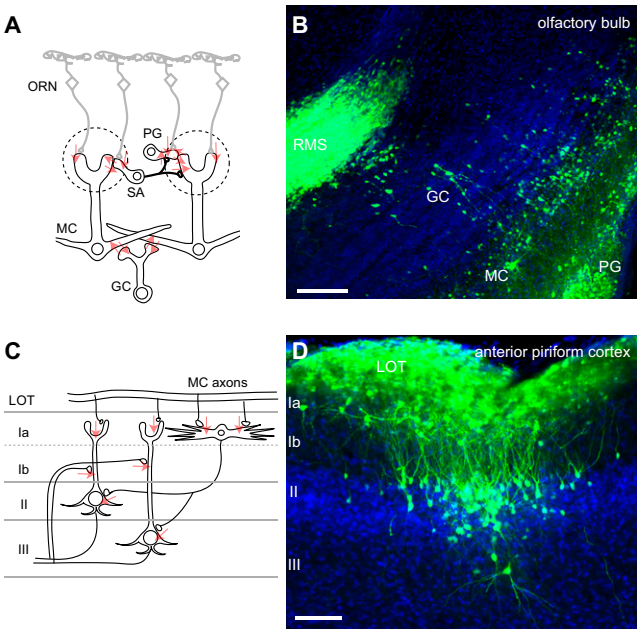

Fig. 4. Labeling of the olfactory system with VSV(LCMV-G). (*A*) Connection diagram (red arrows) from the peripheral ORNs, which were infected in the nose, to the neurons in the OB. SA, short axon cells, MC, mitral cells, GC, granule cells. (*B*) OB at 3 dpi showed labeled PG, MC, GC, and the rostral migratory stream (RMS). (*C*) A connection diagram (red arrows) from the MC axons in the lateral olfactory tract (LOT) to the neurons in the olfactory cortex. Layer Ia neurons are primarily GABAergic local inhibitory neurons, and II/III pyramidal cells receive direct input from MC axons, in addition to feedforward inhibition from layer I inhibitor neurons. (*D*) Labeled layer I inhibitory neurons and layer II/III pyramidal cells at 5 dpi in the anterior piriform cortex. (Scale bars: 100 μm.)

eye. Similar conclusions were drawn from infection of the olfactory neuroepithelium (30), although nonneural routes of entry into the CNS also were observed. Lundh (29) as well as van den Pol et al. (20) used electron microscopy to investigate the location of budding VSV virions in infected neurons. They found that VSV budded from the basolateral surfaces of neurons, but not from their apical surfaces. These data are not in agreement with the observed anterograde spread pattern of WT VSV (29, 30). This discrepancy may be due to differences in the sensitivity of electron microscopy vs. viral transmission.

A chimeric VSV using LCMV-G had been shown to replicate to high titer (11), and one study suggested that virions of a related virus (Lassa virus) are released from the apical surface of infected epithelial cells (31), although another study showed basolateral release of LCMV from airway epithelia (32). Infection of the brain after injection into the eye of VSV(LCMV-G) first led to labeled retinorecipient areas and then several secondary locations in the visual pathway. Cell health could be used as a proxy for order in the circuit. However, WT VSV did not label the brain after infection of the eye, in contrast to the results reported by Lundh (29). Variations in the origin of the G gene may explain this difference. Although we and Lundh (29) used the Indiana serotype of VSV, we used the G gene from the Orsay strain (14), and the strain of VSV used by Lundh was not specified. When injected into the CP, VSV(LCMV-G) labeled cells in the CP, as well as cell bodies in downstream nuclei from the injection site. The number of labeled cells increased over time, but labeled cells remained restricted to this pathway. VSV(LCMV-G) also labeled the brain after injection into the olfactory epithelium. The viral spread in the OB and higher olfactory centers was generally consistent with the anterograde connections of the olfactory system. One exception was the robust labeling of the RMS, which is composed of immature GC and PG precursors. Because they do not form mature synapses, this labeling cannot be explained by viral spread via regular synaptic connections. Because cells in the RMS form specific cell–cell contacts for chain migration (33), the virus may preferentially spread via unique appositions during chain migration. Viral spread beyond the piriform cortex by 5–6 dpi included potential fourth-order neurons of the olfactory pathway, including in the hippocampus. Future studies using monosynaptic transmission coupled with the definition of "starter cells" using TVA (Fig. 5) (34) could clarify the connection diagram from the piriform cortex to these putative fourth-order neurons.

A surprising result was noted when the G-deleted VSV pseudotyped with LCMV-G was injected into the CP. This injection resulted in labeling of cell bodies in the GP and STn, which are a significant distance away from the injection site (3/3 injected animals). This labeling pattern was quite different from a G-deleted VSV pseudotyped with RABV-G, which gave cortical labeling but almost no labeling in the GP ($n = 4$). Cells in the GP and STn are predominately anterograde to the injection site. The G-deleted VSV may have replicated in the CP cells, traveled down the axons of these cells, and infected GP neurons, all without the viral genome encoding the viral glycoprotein. VSV can bud from an infected cell without the G protein in tissue culture (5, 35). In some

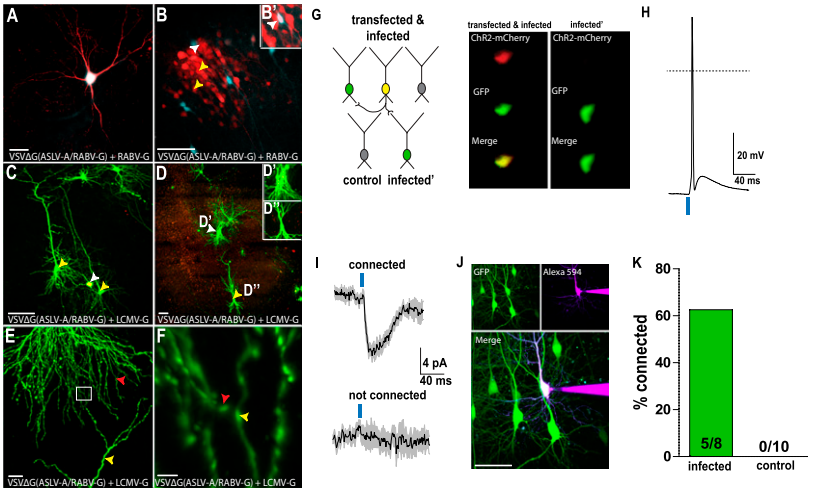

Fig. 5. Recombinant VSV vectors can be used for monosynaptic tracing. Cultured hippocampal slices were used to test for monosynaptic transmission of replication-incompetent VSV after specific infection of TVA-expressing neurons. A gene gun was used to deliver plasmids, as indicated, to test for infectivity of virions pseudotyped by the fusion protein, ASLV-A/RABV-G, as well as transmission using either RABV-G or LCMV-G. (*A* and *B*) Transfected plasmids encoded TVA, CFP (blue, as a transfection marker), and RABV-G. Infection with VSVΔG encoding mCherry pseudotyped with ASLV-A/RABV-G 18 hpi resulted in many more infection events, relative to those seen without TVA. (*A*) An infected (mCherry$^+$) and transfected (CFP$^+$) cell. (*B*) Spread was seen from cells that were both transfected (CFP$^+$) and infected (mCherry$^+$) (white arrowhead) to many cells adjacent to the cell bodies and dendrites (yellow arrowheads) of the transfected cells by 18 hpi. (*B′*) The cell with the white arrowhead in *B* was expressing mCherry. (*C*–*F*) Transfected plasmids encoded TVA, LCMV-G, and ChR2-mCherry. Infection was with VSVΔG encoding GFP. (*C* and *D*) Transfected/infected cells (mCherry$^+$/GFP$^+$, white arrowhead) were observed with infection of nearby nontransfected cells (mCherry$^-$/GFP$^+$, yellow arrowheads). These secondarily infected cells extended dendritic processes to the axon terminals of transfected/ infected cells. *Insets* in *D* show colabel of the mCherry and GFP in the upstream (*D′*), but not downstream (*D″*) neuron. Note that there are relatively fewer clusters of infected cells near the cell body and dendrites of transfected$^+$/infected$^+$ pyramidal cells (*D*) compared with the clusters seen after introduction of RABV-G into pyramidal cells, shown in *B*. (*E* and *F*) Juxtaposition of processes of transfected$^+$/infected$^+$ (red arrowhead) and transfected$^-$/infected$^+$ cells (yellow arrowhead). (*F*) High magnification of boxed area in *E*. (*G*–*K*) Patch clamp recordings were obtained from infected (transfected$^-$/infected$^+$) and control (transfected$^-$/infected$^-$) neurons clustered around upstream (transfected$^+$/infected$^+$) neurons. Upstream neurons were optically activated with pulses of blue light. (*G*) Diagram of recording configuration (*Left*) and images of the schematized upstream and infected cells taken through a camera mounted on the physiology microscope (*Right*). (*H*) Current clamp recordings made from upstream neurons demonstrate that a 2-ms pulse of 20-mW, 473-nm light was sufficient to fire an action potential. (*I*) Example voltage clamp (V_m = −70 mV) from two neurons with (infected) and without (not infected) a synaptic connection to the upstream neuron. Connected cells were identified by inward currents that were reliably evoked and time locked to the optical stimulus. (*J*) Recorded neurons were filled with dye through the patch electrode, and two photon stacks were used to image and confirm the cell's infection status. Example shown was the downstream connected cell in *I*. (*K*) Summary graph showing the percent of connected infected and control (uninfected) neurons. Multiple infected and uninfected cells were recorded from each cluster (six clusters total). (Scale bars: *A*–*D*, *J*, 100 μm; *E*, 20 μm; *F*, 2.5 μm.)

cases, virions without any envelope protein might fuse with a closely juxtaposed membrane, particularly at the synaptic cleft, where there is rapid membrane fusion and recycling. Such fusion occurs for some other enveloped viruses, because PRV without its gD envelope protein is infectious across synapses, whereas HSV-1 is not (36). Because VSV did not transmit after infection with the G-deleted virus pseudotyped by RABV-G, it is possible that residual LCMV-G protein persists from the initial virus infection, permitting the virus to infect an anterograde, connected neuron. Alternatively, the LCMV-G protein, but not RABV-G protein, might enable a phenomenon known as transcytosis. HIV, which is also an enveloped virus, can pass from a cell to its neighbor by using such a mechanism (37, 38). Based on these results from CP injections, replication-incompetent VSV pseudotyped with LCMV-G could thus be explored for use as a monosynaptic tracer, even without the engineering discussed below.

Results presented in this study indicate that VSV with RABV-G or LCMV-G spreads primarily among synaptically connected neurons. To conduct physiological analysis of putative connected pairs, it was necessary to use a virus with a mutant form of the M gene for these experiments (M51R mutant) (25, 26). Because the M protein shuts off host transcription and RNA export, M is thought to be the main component of G-deleted VSV's rapid cytotoxicity (26). This M mutant was thus a good candidate to delay toxicity long enough to allow physiological recordings to be made. With this mutant, synaptic connectivity was observed in 5/8 pairs of infected neurons vs. 0/10 pairs where one neuron was unlabeled. It is likely that greater than 5/8 of the pairs were connected, as there are multiple reasons why currents may not have been successfully recorded. First, synapses in the culture system used are known to be transient (39, 40). In addition, synapses at this stage of development may be "silent" (i.e., containing NMDA receptors but not AMPA receptors) (41). Finally, cell-attached recordings of upstream neurons demonstrated that optical activation was not always sufficient to fire an action potential, likely because of viral toxicity.

Of additional interest is the lack of spread to glia or cells other than mature neurons. This rule is occasionally broken, however, as in the case of the infection of RMS cells. In addition, Muller glial infection has been shown for PRV (42), and RABV has been shown to sometimes infect cortical glia (43). VSV(LCMV-G), PRV, and RABV are thus not exclusively transsynaptic. The reasons for these exceptions are not clear, but likely are due to the close juxtaposition of membranes of certain cell types in particular locations. Furthermore, the exact sequence of a G protein might determine its ability to direct infection of neurons vs. glia. A recent report using the LCMV-G protein from the WE strain of LCMV to pseudotype VSV showed infection of glia, but not neurons (44). The Armstrong strain clone 13 of LCMV-G was used in our study, which likely explains the difference in neuronal vs. glial infection, because a single amino acid change in G can alter receptor binding (45).

An interesting question raised by these patterns of transmission concerns how VSV with these different G proteins enters cells. VSV with its own G protein has a very broad host range, including insects, mammals, and fish (7). Our current understanding of the VSV entry process is that association with the cell likely occurs through electrostatic interactions (46, 47). Whether a specific receptor is engaged in the entry process remains uncertain, but the broad host range suggests a well-conserved molecule or the use of multiple receptors. After binding, tracking of single viral particles into live cells has revealed that the virus is internalized by an altered mode of clathrin-mediated endocytosis (48, 49). In the endocytic pathway, the glycoprotein undergoes a major acid pH-triggered conformational change that catalyzes fusion of the viral and cellular membrane and releases the viral core into the host cell (50, 51). For LCMV, the only defined receptor is α-dystroglycan (52), which is broadly expressed in the nervous system. The fact that most or all cells within a pathway seem to be infectable implies that all cells have an LCMV-G receptor, which is possible. Alternatively, transmission among cells across a synaptic cleft might be independent of a specific receptor, and the role of LCMV-G might be to target efficient budding to the presynaptic surface. This model is not meant to be an exclusive one, as clearly receptor-specific/receptor-mediated entry of virions can also occur, e.g., TVA-EnvA entry events (15, 53, 54). Further studies of

the pathways for both viral egress and entry may provide a foundation for understanding the fortuitous observation that changes in the G protein can lead to nearly exclusive transsynaptic transmission in specific directions.

Materials and Methods

Virus Construction and Production. All methods were those described previously. For details, see *SI Materials and Methods*.

Injections of Mice. All mouse work was conducted in biosafety containment level 2 conditions and was approved by the Longwood Medical Area Institutional Animal Care and Use Committee.

Injection details are provided in *SI Materials and Methods*.

Hippocampal Slice Cultures. For all methods for slice cultures and whole-cell recordings, see *SI Materials and Methods*.

ACKNOWLEDGMENTS. We thank Botond Roska, Ed Callaway, Rami Burstein, Klaus Conzelmann, Jojo Nassi, Vanessa Kainz, Enrica Strettoi, Elio Raviola, Philip Kranzusch, and Amy S. Lee for informative discussions regarding viral tracing; Jonathan Tang for technical assistance; David Cardozo, Rick Born, and Vladimir Berezovskii for help with neuroanatomy; and Ed Callaway for gifts of plasmids. This work was supported by the Howard Hughes Medical Institute (C.L.C., L.L., and B.S.) and Grants AI081842 (to S.P.J.W.) and NS068012-01 (to K.T.B.).

1. Enquist L-W, Card J-P (2003) Recent advances in the use of neurotropic viruses for circuit analysis. *Curr Opin Neurobiol* 13:603–606.
2. Kelly R-M, Strick P-L (2000) Rabies as a transneuronal tracer of circuits in the central nervous system. *J Neurosci Methods* 103:63–71.
3. Enquist L-W (2002) Exploiting circuit-specific spread of pseudorabies virus in the central nervous system: Insights to pathogenesis and circuit tracers. *J Infect Dis* 186(Suppl 2):S209–S214.
4. Sun X, Belouzard S, Whittaker G-R (2008) Molecular architecture of the bipartite fusion loops of vesicular stomatitis virus glycoprotein G, a class III viral fusion protein. *J Biol Chem* 283:6418–6427.
5. Mebatsion T, Konig M, Conzelmann K-K (1996) Budding of rabies virus particles in the absence of the spike glycoprotein. *Cell* 84:941–951.
6. Bates P, Young J-A, Varmus H-E (1993) A receptor for subgroup A Rous sarcoma virus is related to the low density lipoprotein receptor. *Cell* 74:1043–1051.
7. Lyles D-S (2007) *Virology* (Lippincott Williams & Wilkins, New York), pp 1363–1408.
8. van den Pol A-N, et al. (2009) Viral strategies for studying the brain, including a replication-restricted self-amplifying delta-G vesicular stomatis virus that rapidly expresses transgenes in brain and can generate a multicolor golgi-like expression. *J Comp Neurol* 516:456–481.
9. Kretzschmar E, Buonocore L, Schnell M-J, Rose J-K (1997) High-efficiency incorporation of functional influenza virus glycoproteins into recombinant vesicular stomatitis viruses. *J Virol* 71:5982–5989.
10. Perez M, Watanabe M, Whitt M-A, de la Torre J-C (2001) N-terminal domain of Borna disease virus G (p56) protein is sufficient for virus receptor recognition and cell entry. *J Virol* 75:7078–7085.
11. Pinschewer D-D, et al. (2004) Kinetics of protective antibodies are determined by the viral surface antigen. *J Clin Invest* 114:988–993.
12. Roberts A, Buonocore L, Price R, Forman J, Rose J-K (1999) Attenuated vesicular stomatitis viruses as vaccine vectors. *J Virol* 73:3723–3732.
13. Tatsuo H, et al. (2000) Virus entry is a major determinant of cell tropism of Edmonston and wild-type strains of measles virus as revealed by vesicular stomatitis virus pseudotypes bearing their envelope proteins. *J Virol* 74:4139–4145.
14. Whelan S-P, Ball L-A, Barr J-N, Wertz G-T (1995) Efficient recovery of infectious vesicular stomatitis virus entirely from cDNA clones. *Proc Natl Acad Sci USA* 92:8388–8392.
15. Wickersham IR, et al. (2007) Monosynaptic restriction of transsynaptic tracing from single, genetically targeted neurons. *Neuron* 53:639–647.
16. Beier K-T, Samson M-E, Matsuda T, Cepko C-L (2011) Conditional expression of the TVA receptor allows clonal analysis of descendents from Cre-expressing progenitor cells. *Dev Biol* 353:309–320.
17. Pickard G-E, et al. (2002) Intravitreal injection of the attenuated pseudorabies virus PRV Bartha results in infection of the hamster suprachiasmatic nucleus only by retrograde transsynaptic transport via autonomic circuits. *J Neurosci* 22:2701–2710.
18. Greferath U, Kambourakis M, Barth C, Fletcher E-L, Murphy M (2009) Characterization of histamine projections and their potential cellular targets in the mouse retina. *Neuroscience* 158:932–944.
19. Wang Q, Burkhalter A (2007) Area map of mouse visual cortex. *J Comp Neurol* 502:339–357.
20. van den Pol A-N, Dalton K-P, Rose J-K (2002) Relative neurotropism of a recombinant rhabdovirus expressing a green fluorescent envelope glycoprotein. *J Virol* 76:1309–1327.
21. Shepherd G (2004) *The Synaptic Organization of the Brain* (Oxford University Press, New York).
22. Willhite D-C, et al. (2006) Viral tracing identifies distributed columnar organization in the olfactory bulb. *Proc Natl Acad Sci USA* 103:12592–12597.
23. Stokes C-C, Isaacson J-S (2010) From dendrite to soma: Dynamic routing of inhibition by complementary interneuron microcircuits in olfactory cortex. *Neuron* 67:452–465.
24. Astic L, Saucier D, Coulon P, Lafay F, Flamand A (1993) The CVS strain of rabies virus as transneuronal tracer in the olfactory system of mice. *Brain Res* 619:146–156.
25. Ahmed M, Lyles D-S (1997) Identification of a consensus mutation in M protein of vesicular stomatitis virus from persistently infected cells that affects inhibition of host-directed gene expression. *Virology* 237:378–388.
26. Hoffmann M, et al. (2010) Fusion-active glycoprotein G mediates the cytotoxicity of vesicular stomatitis virus M mutants lacking host shut-off activity. *J Gen Virol* 91:2782–2793.
27. Thomas D-C, Brewer C-B, Roth M-G (1993) Vesicular stomatitis virus glycoprotein contains a dominant cytoplasmic basolateral sorting signal critically dependent upon a tyrosine. *J Biol Chem* 268:3313–3320.
28. Krnjević K, Silver A (1965) A histochemical study of cholinergic fibres in the cerebral cortex. *J Anat* 99:711–759.
29. Lundh B (1990) Spread of vesicular stomatitis virus along the visual pathways after retinal infection in the mouse. *Acta Neuropathol* 79:395–401.
30. Plakhov I-V, Arlund E-E, Aoki C, Reiss C-S (1995) The earliest events in vesicular stomatitis virus infection of the murine olfactory neuroepithelium and entry of the central nervous system. *Virology* 209:257–262.
31. Schlie K, et al. (2010) Viral protein determinants of Lassa virus entry and release from polarized epithelial cells. *J Virol* 84:3178–3188.
32. Dylla D-E, Michele D-E, Campbell K-P, McCray P-B, Jr. (2008) Basolateral entry and release of New and Old World arenaviruses from human airway epithelia. *J Virol* 82:6034–6038.
33. Lois C, García-Verdugo J-M, Alvarez-Buylla A (1996) Chain migration of neuronal precursors. *Science* 271:978–981.
34. Miyamichi K, et al. (2011) Cortical representations of olfactory input by trans-synaptic tracing. *Nature* 472:191–196.
35. Schnitzer T-J, Dickson C, Weiss R-A (1979) Morphological and biochemical characterization of viral particles produced by the tsO45 mutant of vesicular stomatitis virus at restrictive temperature. *J Virol* 29:185–195.
36. Ch'ng T-H, Spear P-G, Struyf F, Enquist L-W (2007) Glycoprotein D-independent spread of pseudorabies virus infection in cultured peripheral nervous system neurons in a compartmented system. *J Virol* 81:10742–10757.
37. Mothes W, Sherer N-M, Jin J, Zhong P (2010) Virus cell-to-cell transmission. *J Virol* 84:8360–8368.
38. Bomsel M (1997) Transcytosis of infectious human immunodeficiency virus across a tight human epithelial cell line barrier. *Nat Med* 3:42–47.
39. Nägerl U-V, Eberhorn N, Cambridge S-B, Bonhoeffer T (2004) Bidirectional activity-dependent morphological plasticity in hippocampal neurons. *Neuron* 44:759–767.
40. Tashiro A, Yuste R (2004) Regulation of dendritic spine motility and stability by Rac1 and Rho kinase: evidence for two forms of spine motility. *Mol Cell Neurosci* 26:429–440.
41. Montgomery J-M, Pavlidis P, Madison D-V (2001) Pair recordings reveal all-silent synaptic connections and the postsynaptic expression of long-term potentiation. *Neuron* 29:691–701.
42. Viney T-J, et al. (2007) Local retinal circuits of melanopsin-containing ganglion cells identified by transsynaptic viral tracing. *Curr Biol* 17:981–988.
43. Marshel J-H, Mori T, Nielsen K-J, Callaway E-M (2010) Targeting single neuronal networks for gene expression and cell labeling in vivo. *Neuron* 67:562–574.
44. Muik A, et al. (2011) Pseudotyping vesicular stomatitis virus with lymphocytic choriomeningitis virus glycoproteins enhances infectivity for glioma cells and minimizes neurotropism. *J Virol* 85:5679–5684.
45. Sullivan B-M, et al. (2011) Point mutation in the glycoprotein of lymphocytic choriomeningitis virus is necessary for receptor binding, dendritic cell infection, and long-term persistence. *Proc Natl Acad Sci USA* 108:2969–2974.
46. Wunner W-H, Reagan K-J, Koprowski H (1984) Characterization of saturable binding sites for rabies virus. *J Virol* 50:691–697.
47. Bailey C-A, Miller D-K, Lenard J (1984) Effects of DEAE-dextran on infection and hemolysis by VSV. Evidence that nonspecific electrostatic interactions mediate effective binding of VSV to cells. *Virology* 133:111–118.
48. Cureton D-K, Massol R-H, Saffarian S, Kirchhausen T-L, Whelan S-P-J (2009) Vesicular stomatitis virus enters cells through vesicles incompletely coated with clathrin that depend upon actin for internalization. *PLoS Pathog* 5:e1000394.
49. Johannsdottir H-K, Mancini R, Kartenbeck J, Amato L, Helenius A (2009) Host cell factors and functions involved in vesicular stomatitis virus entry. *J Virol* 83:440–453.
50. Roche S, Bressanelli S, Rey F-A, Gaudin Y (2006) Crystal structure of the low-pH form of the vesicular stomatitis virus glycoprotein G. *Science* 313:187–191.
51. Roche S, Rey F-A, Gaudin Y, Bressanelli S (2007) Structure of the prefusion form of the vesicular stomatitis virus glycoprotein G. *Science* 315:843–848.
52. Cao W, et al. (1998) Identification of alpha-dystroglycan as a receptor for lymphocytic choriomeningitis virus and Lassa fever virus. *Science* 282:2079–2081.
53. Delos S-E, Godby J-A, White J-M (2005) Receptor-induced conformational changes in the SU subunit of the avian sarcoma/leukosis virus A envelope protein: implications for fusion activation. *J Virol* 79:3488–3499.
54. Narayan S, Barnard R-J-O, Young J-A-T (2003) Two retroviral entry pathways distinguished by lipid raft association of the viral receptor and differences in viral infectivity. *J Virol* 77:1977–1983.
55. Stoppini L, Buchs P-A, Muller D (1991) A simple method for organotypic cultures of nervous tissue. *J Neurosci Methods* 37:173–182.
56. Franklin K, Paxinos G (1997) *The Mouse Brain in Stereotaxic Coordinates* (Academic Press, San Diego).